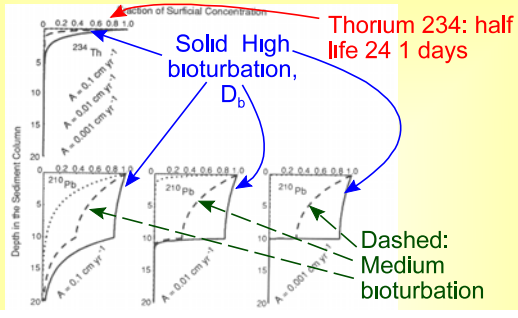
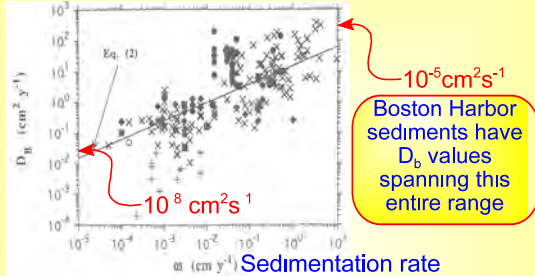
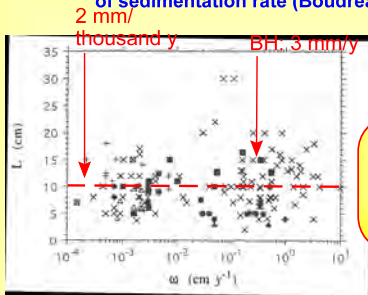


<div data-bbox="267 205 753 363" data-label="Section-Header"> <h2>Bioturbation <End> & Microphytobenthos, especially Benthic Diatom Production</h2> </div> <div data-bbox="339 375 673 403" data-label="Text"> <p>Class 5: Tu September 16, 2008</p> </div> <div data-bbox="656 510 771 537" data-label="Text"> <p>EEOS630</p> </div>	<div data-bbox="818 130 1255 205" data-label="Section-Header"> <h3>Slide 1 Bioturbation <End> & Microphytobenthos, especially</h3> </div> <div data-bbox="818 228 1180 262" data-label="Text"> <p>Benthic Diatom Production</p> </div> <div data-bbox="818 352 941 386" data-label="Text"> <p>NOTES:</p> </div>
<div data-bbox="389 690 625 724" data-label="Section-Header"> <h3>Class schedule</h3> </div> <div data-bbox="431 737 579 762" data-label="Section-Header"> <h4>Order of topics</h4> </div> <div data-bbox="222 751 737 1050" data-label="List-Group"> <ul style="list-style-type: none"> • Microphytobenthos <ul style="list-style-type: none"> ▸ Chapter 3 ▸ Gould, D. G. and E. D. Gallagher. 1990. Field measurement of specific growth rate, biomass and primary production of benthic diatoms of Savin Hill Cove, Boston. Limnol. Oceanogr. 35: 1757-1770. • For Thursday Benthic Population Biology <ul style="list-style-type: none"> ▸ Gallagher, E. D., G. B. Gardner and P. A. Jumars 1990. Competition among the pioneers in soft bottom benthic succession: field experiments and analysis of the Gilpin-Ayala competition model. Oecologia 83: 427-442. ▸ Whitlatch, R. B. 1980. Patterns of resource utilization and coexistence in marine intertidal deposit-feeding communities. J. Mar. Res. 38: 743-765. </div> <div data-bbox="656 1037 771 1064" data-label="Text"> <p>EEOS630</p> </div>	<div data-bbox="818 657 1143 690" data-label="Section-Header"> <h3>Slide 2 Class schedule</h3> </div> <div data-bbox="818 779 941 812" data-label="Text"> <p>NOTES:</p> </div>
<div data-bbox="285 1180 742 1215" data-label="Section-Header"> <h3>Estimating sedimentation rates</h3> </div> <div data-bbox="302 1226 716 1253" data-label="Text"> <p>& sediment-mixing rates, Pb-210 22-y half life</p> </div> <div data-bbox="243 1245 709 1554" data-label="Figure"> <p>If porosity constant, Sediment accumulation = $\lambda(z_2 - z_1) / (\ln [A_{z_1} / A_{z_2}])$</p> </div>	<div data-bbox="818 1148 1367 1182" data-label="Section-Header"> <h3>Slide 3 Estimating sedimentation rates</h3> </div> <div data-bbox="818 1268 941 1302" data-label="Text"> <p>NOTES:</p> </div>

<p>Typical bioturbation profiles</p> <p>Jumars (1993): But what controls D_b & L?</p>  <p>Section of Surficial Concentration</p> <p>Thorium 234: half life 24.1 days</p> <p>Solid High bioturbation, D_b</p> <p>Dashed: Medium bioturbation</p>	<p>Slide 4 Typical bioturbation profiles</p> <p>NOTES:</p>
<p>What are typical values for D_b?</p> <p>Goldberg-Koide Equation:</p> $\frac{\partial A}{\partial t} = \frac{\partial}{\partial z} \left[D_b \frac{\partial A}{\partial z} \right] - \omega \frac{\partial A}{\partial z} - \lambda A$ <ul style="list-style-type: none"> Deep-sea and nearly azoic polluted sediments: $10^{-6} \text{ cm}^2 \text{ s}^{-1}$ Exceptionally high rates of bioturbation in coastal zones with conveyor-belt feeders: $2 \times 10^{-5} \text{ cm}^2 \text{ s}^{-1}$ By comparison <ul style="list-style-type: none"> Horizontal eddy diffusion $K_x > 10^6 \text{ cm}^2 \text{ s}^{-1}$ Vertical eddy diffusion, K_z: $0.05 - 4 \text{ cm}^2 \text{ s}^{-1}$ Molecular diffusion coefficients for O_2 & CO_2 $\approx 2 \times 10^{-5} \text{ cm}^2 \text{ s}^{-1}$ 	<p>Slide 5 What are typical values for D_b?</p> <p>NOTES:</p>
<p>Bioturbation = f(Sedimentation)</p> <p>Boudreau (1994): Bioturbation (D_b) & sedimentation (ω)</p>  <p>$10^{-5} \text{ cm}^2 \text{ s}^{-1}$</p> <p>$10^{-8} \text{ cm}^2 \text{ s}^{-1}$</p> <p>Boston Harbor sediments have D_b values spanning this entire range</p> <p>Sedimentation rate</p>	<p>Slide 6 Bioturbation = f(Sedimentation)</p> <p>NOTES:</p>

Mixed Layer vs. Sedimentation

Bioturbation depth (L), 10-cm average, is **not** a function of sedimentation rate (Boudreau 1994)



EEOS630

Slide 7 Mixed Layer vs. Sedimentation

NOTES:

D_b increases with sedimentation, but so too does the rate at which organic matter degrades

Boudreau (1994): the relationship between bioturbation rate, D_b , and sedimentation rate, w :

$$D_b = 15.7 w^{0.6}$$

Tromp et al. (1994): the relationship between the rate of degradation of organic matter with reaction rate k and sedimentation rate w :

$$k = 3.0 w^{0.6}$$

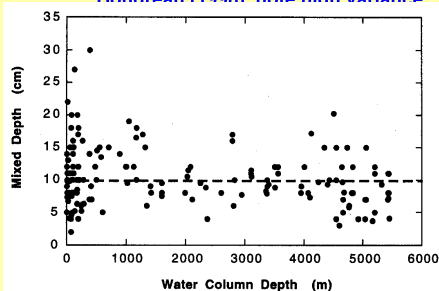
The 0.6 exponents cancel out when inserted in a model to predict mixed layer depth (Boudreau 1998, equations (5) & (6)). So, at shallower depths there is more organic matter input, but this higher organic matter input is associated with higher degradation and bioturbation rates producing similar depths of available food. Animals feed where there is available food.

Slide 8 D_b increases with sedimentation, but so too does the rate at which organic matter degrades

NOTES:

Global 10-cm depth average

Boudreau (1998) note high variance



EEOS630

Slide 9 Global 10-cm depth average

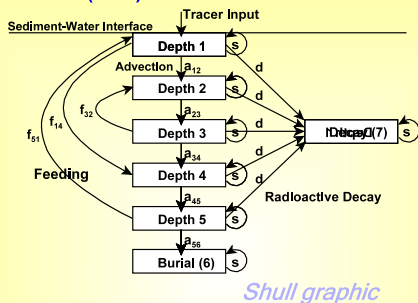
NOTES:

<div data-bbox="363 168 656 207" data-label="Section-Header"> <h3>Other explanations</h3> </div> <div data-bbox="238 243 656 525" data-label="List-Group"> <ul style="list-style-type: none"> • Predation: depth of fish feeding <ul style="list-style-type: none"> ▸ How deep can a flounder bite? ▸ How deep can a crab dig? • Compaction of mud • Relationship to microphytobenthic & phytodetrital food caching? <ul style="list-style-type: none"> ▸ Food caching (see Gallagher & Keay 1998) ▸ Storing food from the surface in subsurface burrows for later ingestion </div> <div data-bbox="656 514 771 541" data-label="Text"> <p>EEOS630</p> </div>	<div data-bbox="816 132 1222 172" data-label="Section-Header"> <h3>Slide 10 Other explanations</h3> </div> <div data-bbox="816 256 940 291" data-label="Text"> <p>NOTES:</p> </div>
<div data-bbox="272 648 751 688" data-label="Text"> <p>Guinasso & Schink (1975) modeled a pulse of glass microtektites (glass spheres) and introduced G a dimensionless number</p> </div> <div data-bbox="284 693 743 741" data-label="Text"> <p>Major implications for pollution, e.g., New Bedford PCBs or LA's DDT</p> </div> <div data-bbox="230 741 751 1024" data-label="Figure"> </div>	<div data-bbox="816 621 1344 770" data-label="Section-Header"> <h3>Slide 11 Guinasso & Schink (1975) modeled a pulse of glass microtektites (glass spheres) and introduced G a dimensionless number</h3> </div> <div data-bbox="816 854 940 890" data-label="Text"> <p>NOTES:</p> </div>
<div data-bbox="310 1255 712 1295" data-label="Section-Header"> <h3>Modeling non-local mixing</h3> </div> <div data-bbox="410 1299 584 1329" data-label="Text"> <p>Boudreau (1986b)</p> </div> <div data-bbox="233 1333 656 1467" data-label="Text"> <p><i>"Infaunal macroorganisms are capable of exchanging sedimentary material over distances equal to or greater than the scale over which the concentration of tracer changes substantially. This type of non-diffusive bioturbation is called nonlocal mixing."</i></p> </div> <div data-bbox="230 1467 727 1617" data-label="Image"> </div>	<div data-bbox="816 1222 1328 1262" data-label="Section-Header"> <h3>Slide 12 Modeling non-local mixing</h3> </div> <div data-bbox="816 1344 940 1379" data-label="Text"> <p>NOTES:</p> </div>

<div data-bbox="310 165 708 199" data-label="Section-Header"> <h3>Lowes Cove Maine mudflat</h3> </div> <div data-bbox="303 214 721 258" data-label="Text"> <p><i>Leitoscoloplos</i>, a conveyor belt feeder, called <i>Scoloplos</i> spp. in Rice (1986)</p> </div> <div data-bbox="230 262 578 516" data-label="Image"> </div> <div data-bbox="594 264 760 495" data-label="Text"> <p>Rice (1986) JMR Modelled bioturbation as if only 1 species, <i>Leitoscoloplos</i> was responsible</p> </div> <div data-bbox="656 510 771 537" data-label="Text"> <p>EEOS630</p> </div>	<div data-bbox="818 132 1336 165" data-label="Section-Header"> <h3>Slide 13 Lowes Cove Maine mudflat</h3> </div> <div data-bbox="818 254 940 287" data-label="Text"> <p>NOTES:</p> </div>
<div data-bbox="310 653 712 688" data-label="Section-Header"> <h3>Subduction of a chalk layer</h3> </div> <div data-bbox="279 699 747 726" data-label="Text"> <p>Rice 1986: <i>Leitoscoloplos</i> is a conveyor-belt feeder</p> </div> <div data-bbox="250 726 574 940" data-label="Figure"> </div> <div data-bbox="422 789 680 861" data-label="Equation-Block"> $\frac{\partial A}{\partial t} = \frac{\partial}{\partial z} \left[D_b \frac{\partial A}{\partial z} \right] - \omega \frac{\partial A}{\partial z} - \lambda A$ </div> <div data-bbox="305 951 592 1018" data-label="Text"> <p>Rice (1986) modeled bioturbation with an advection term, bioadvection, not biodiffusion D_b</p> </div> <div data-bbox="656 999 771 1024" data-label="Text"> <p>EEOS630</p> </div>	<div data-bbox="818 621 1336 655" data-label="Section-Header"> <h3>Slide 14 Subduction of a chalk layer</h3> </div> <div data-bbox="818 743 940 777" data-label="Text"> <p>NOTES:</p> </div>
<div data-bbox="276 1142 751 1178" data-label="Section-Header"> <h3>Rice's (1986) bioturbation model</h3> </div> <div data-bbox="418 1188 581 1215" data-label="Text"> <p>^7Be, 55-d half-life</p> </div> <div data-bbox="222 1215 574 1425" data-label="Figure"> </div> <div data-bbox="225 1428 579 1467" data-label="Caption"> <p>Figure 9. Be-7 depth profile at station 84-6 and theoretical transient-state profile generated by assuming a constant surface concentration (4.62 dpm · g⁻¹) and time-varying biodeposition rate by <i>Scoloplos</i> (inset illustration).</p> </div> <div data-bbox="574 1218 751 1423" data-label="Text"> <p>Rice's ^7Be profile could not be modeled adequately using the diffusive Goldberg Koide equation</p> </div> <div data-bbox="355 1457 617 1520" data-label="Equation-Block"> $\frac{\partial A}{\partial t} = \frac{\partial}{\partial z} \left[D_b \frac{\partial A}{\partial z} \right] - \omega \frac{\partial A}{\partial z} - \lambda A$ </div> <div data-bbox="656 1486 771 1514" data-label="Text"> <p>EEOS630</p> </div>	<div data-bbox="818 1110 1408 1144" data-label="Section-Header"> <h3>Slide 15 Rice's (1986) bioturbation model</h3> </div> <div data-bbox="818 1232 940 1266" data-label="Text"> <p>NOTES:</p> </div>

Shull's Bioturbation Model

Shull (2001): Realistic bioturbation modeling



Slide 16 Shull's Bioturbation Model

NOTES:

Bioturbation Transition Matrix

Shull's finite Markov chain, a single matrix

From \ To	State at time t	1	2	3	4	5	Burial	Decay
1	s	$a_{12}(1-d)$	0	$f_{14}(1-d)$	0	0	0	d
2	0	s	$a_{23}(1-d)$	0	0	0	0	d
3	0	$f_{32}(1-d)$	s	$a_{34}(1-d)$	0	0	0	d
4	0	0	0	s	$a_{45}(1-d)$	0	0	d
5	$f_{51}(1-d)$	0	0	0	s	$a_{56}(1-d)$	0	d
Burial	0	0	0	0	0	1	0	0
Decay	0	0	0	0	0	0	0	1

Shull graphic

Slide 17 Bioturbation Transition Matrix

NOTES:

Model Equations and Solutions

Solutions from Kemeny & Snell's (1976) Finite Markov chains, can be solved with a very short Matlab program (a potential Project for this class)

Solutions

$$N_t = N_0 P^t$$

$$N_{steady-state} = f(I - Q)^{-1}$$

f = tracer flux, Q = depth submatrix

Tracer Application

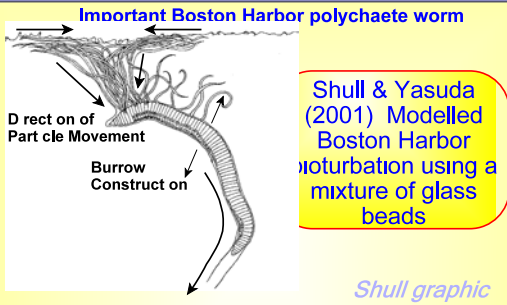
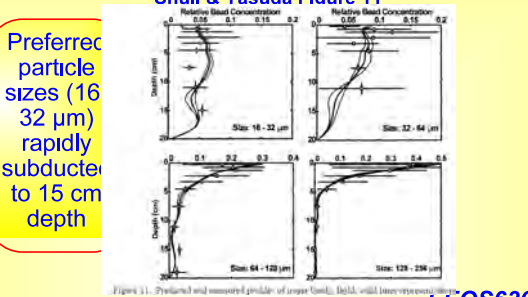
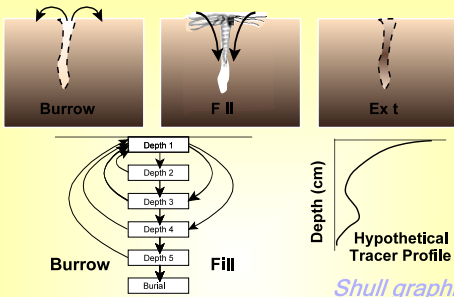
Nonreactive Tracers

Radionuclide Tracers

Shull graphic

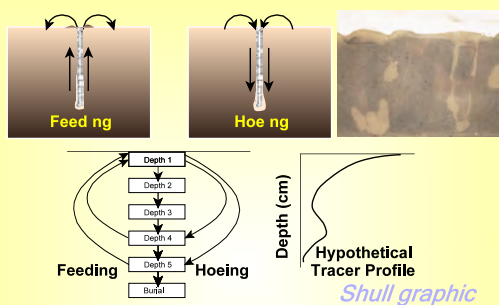
Slide 18 Model Equations and Solutions

NOTES:

<p>Cirratulid feeding: Non-local mixing</p>  <p>Important Boston Harbor polychaete worm</p> <p>Direction of Particle Movement</p> <p>Burrow Construction</p> <p>Shull & Yasuda (2001) Modelled Boston Harbor bioturbation using a mixture of glass beads</p> <p>Shull graphic</p>	<p>Slide 19 Cirratulid feeding: Non-local mixing</p> <p>NOTES:</p>
<p>Size-selective bioturbation</p>  <p>Shull & Yasuda Figure 11</p> <p>Preferred particle sizes (16-32 µm) rapidly subducted to 15 cm depth</p> <p>Figure 11. Preferred and observed profiles of coarse (solid) and fine (dashed) particles. Depth (cm) is on the y-axis. Relative Bead Concentration is on the x-axis. Size: 16 - 32 µm, Size: 32 - 64 µm, Size: 64 - 128 µm, Size: 128 - 256 µm.</p> <p>EEOS630</p>	<p>Slide 20 Size-selective bioturbation</p> <p>NOTES:</p>
<p>Polycirrus eximius: relict burrows</p> <p>Important in Narragansett Bay</p>  <p>Burrow</p> <p>F II</p> <p>Ex t</p> <p>Depth 1</p> <p>Depth 2</p> <p>Depth 3</p> <p>Depth 4</p> <p>Depth 5</p> <p>Burrow</p> <p>Fill</p> <p>Depth (cm)</p> <p>Hypothetical Tracer Profile</p> <p>Shull graphic</p>	<p>Slide 21 Polycirrus eximius: relict burrows</p> <p>NOTES:</p>

Non-local feeding, hoeing & food caching

Shull (2000, 2001), see also Gallagher & Keay (1998)

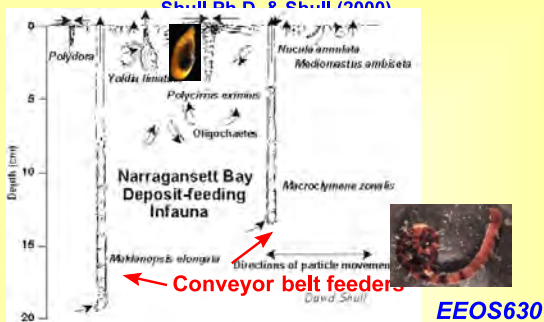


Slide 22 Non-local feeding, hoeing & food caching

NOTES:

Narragansett Bay benthos

Shull 2000 & Shull (2000)

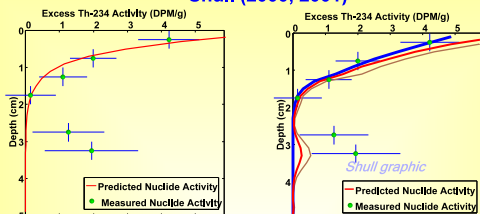


Slide 23 Narragansett Bay benthos

NOTES:

Traditional models vs. Non-local

Shull (2000, 2001)



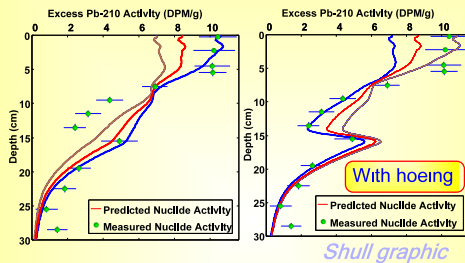
Goldberg Koide bioturbation model is a poor fit to the data and would tremendously overestimate the amount of sediment moved

Slide 24 Traditional models vs. Non-local

NOTES:

To hoe or not to hoe

Better fit if 40% of particles ingested by maldanid polychaetes (bamboo worms) was collected at the sediment-water interface



Slide 25 To hoe or not to hoe

NOTES:

^{13}C diatom fluff experiment

Blair et al. (1996), Levin et al. (1997), Levin et al. (1999)

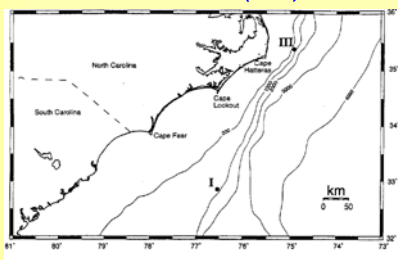


Fig. 1. Location of study sites on the North Carolina margin. Both sites are located to 850 m water depth.

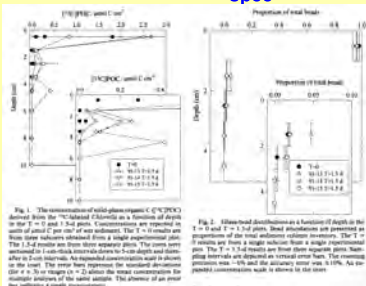
EEOS630

Slide 26 ^{13}C diatom fluff experiment

NOTES:

Blair et al. C-13 fluff experiment

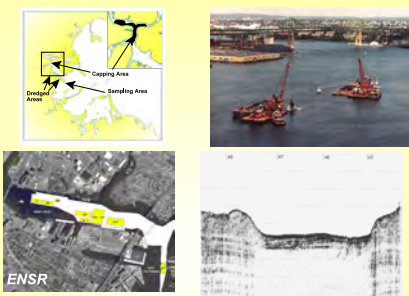
Note C-13 is a stable isotope, measured with Mass spec

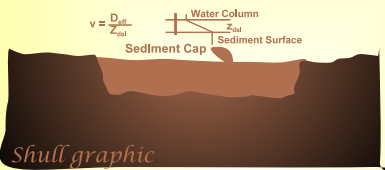


EEOS630

Slide 27 Blair et al. C-13 fluff experiment

NOTES:

<p>Non-local transport modes for fresh organic matter</p> <p>From Blair <i>et al.</i> (1996), Levin <i>et al.</i> 1997 & 1999</p> <ul style="list-style-type: none"> Smith <i>et al.</i> 1986-1987 invoked subsurface defecation to explain naturally occurring 239-,240-Pu profiles in NW Atlantic sediments Graf (1989) explained subsurface Chl <i>a</i> peaks in the deep sea Wheatcroft (1992) Santa Catalina basin beads <ul style="list-style-type: none"> Possibly sediment-tagged Nobel metals in MA Bay "Alternatively, subsurface defecation may be a means of caching material for later use (Jumars <i>et al.</i> 1990, Smith 1994)" Scraping or hoeing surficial material into burrows, as has been observed in shallow water (Dobbs and Whittach 1992) may be another means of rapid transport <p>EEOS630</p>	<p>Slide 28 Non-local transport modes for fresh organic matter</p> <p>NOTES:</p>
<p>Confined Aquatic Disposal (CAD)</p>  <p>ENSR</p>	<p>Slide 29 Confined Aquatic Disposal (CAD)</p> <p>NOTES:</p>
<p>Capping contaminated sediments: Benthic ecological issues for confined aquatic disposal (CAD)</p> <ul style="list-style-type: none"> What currency should be used to assess the need for a cap Where should the CAD cells be placed? Impacts during CAD creation Whether to cap How thick to cap How to monitor <p>EEOS630</p>	<p>Slide 30 Capping contaminated sediments: Benthic ecological issues for confined aquatic disposal (CAD)</p> <p>NOTES:</p>

<div data-bbox="354 165 667 203" data-label="Section-Header"> <h3>Whether to cap cells</h3> </div> <div data-bbox="315 212 725 237" data-label="Section-Header"> <h4>Sedimentation rate, toxicity of new material</h4> </div> <div data-bbox="238 241 662 501" data-label="List-Group"> <ul style="list-style-type: none"> • Reasons to cap <ul style="list-style-type: none"> ▸ Highly toxic material (e.g., dioxin) ▸ Low sedimentation rate ▸ Vulnerable ecological resources ▸ Bet hedging (ecological uncertainty) ▸ Deep bioturbation • Reasons not to cap <ul style="list-style-type: none"> ▸ High natural sedimentation rate ▸ Contaminated ambient surrounding sediment ▸ Ambient community already heavily degraded ▸ Rapid pollutant degradation rate </div> <div data-bbox="657 512 771 537" data-label="Text"> <p>EEOS630</p> </div>	<div data-bbox="818 132 1237 168" data-label="Section-Header"> <h3>Slide 31 Whether to cap cells</h3> </div> <div data-bbox="818 254 940 287" data-label="Text"> <p>NOTES:</p> </div>
<div data-bbox="381 653 638 690" data-label="Section-Header"> <h3>How thick to cap</h3> </div> <div data-bbox="303 699 730 724" data-label="Section-Header"> <h4>Assessing bioturbation & chemical gradients</h4> </div> <div data-bbox="238 728 644 1010" data-label="List-Group"> <ul style="list-style-type: none"> • Natural sediment transport depth • Cap thickness depends on chemical properties of pollutant <ul style="list-style-type: none"> ▸ K_{oc} ▸ Degradation rate • Factors controlling bioturbation rate <ul style="list-style-type: none"> ▸ Biogeography ▸ Food supply and quality ▸ Grain size </div> <div data-bbox="657 999 771 1024" data-label="Text"> <p>EEOS630</p> </div>	<div data-bbox="818 619 1192 655" data-label="Section-Header"> <h3>Slide 32 How thick to cap</h3> </div> <div data-bbox="818 741 940 774" data-label="Text"> <p>NOTES:</p> </div>
<div data-bbox="315 1138 704 1203" data-label="Section-Header"> <h3>Processes affected by cap thickness</h3> </div> <div data-bbox="238 1224 652 1514" data-label="Figure"> <p>Equations</p> $k = f_{oc} k_{oc} C_{sed}$ $D_{eff} = \frac{D_{sed} b}{1+k}$ $v = \frac{D_{eff}}{Z_{sed}}$  <p>Shull graphic</p> </div> <div data-bbox="657 1488 771 1514" data-label="Text"> <p>EEOS630</p> </div>	<div data-bbox="818 1108 1300 1178" data-label="Section-Header"> <h3>Slide 33 Processes affected by cap thickness</h3> </div> <div data-bbox="818 1266 940 1299" data-label="Text"> <p>NOTES:</p> </div>

<div data-bbox="240 163 760 541"> <h3>Effects of bioturbation</h3> <p>Function of (k_{oc}, bioturbation rate, bioturbation depth)</p> <p><i>Shull graphic</i></p> <p>Low k_{oc} (10^4) material diffuses into the water column High k_{oc} (10^6) PCB's, DDE) material remains bound to organic matter</p> <p>EEOS630</p> </div>	<div data-bbox="824 132 1266 168"> <h3>Slide 34 Effects of bioturbation</h3> </div> <div data-bbox="824 258 938 289"> <p>NOTES:</p> </div>
---	--

<p>Methods for estimating Benthic diatom standing stock, production & specific growth rate (μ)</p> <ul style="list-style-type: none"> Estimating standing stock: <ul style="list-style-type: none"> Cell numbers Biomass using Chl a extraction (measured using fluorescence in laboratory) Estimating production <ul style="list-style-type: none"> ^{14}C incorporation into organic matter O_2 production <ul style="list-style-type: none"> Bell jars Microelectrodes Fluorescence: FRR & PAM Estimating μ: Redalje-Laws Chl a-specific ^{14}C activity 	<p>Slide 37 Methods for estimating Benthic diatom standing stock, production & specific growth rate (μ)</p> <p>NOTES:</p>
<p>'μ' μ and little 'r'</p> <p>μ is per capita growth rate; μ_{\max} is max growth rate, intrinsic growth rate, Malthusian parameter</p> $\frac{dN}{dt} = \mu N.$ $\mu = \frac{1}{N} \frac{dN}{dt}.$ $\frac{dN}{dt} = \mu_{\max} N, \text{ with no resource limitation.}$ $\mu_{\max} = \frac{1}{N} \frac{dN}{dt}.$ <p>EEOS630</p>	<p>Slide 38 'μ' μ and little 'r'</p> <p>NOTES:</p>
<p>The Malthusian parameter: r_{\max}</p> <p>Maximum growth rate. no density-dependent limitation</p> $\frac{dN}{dt} = r N.$ $\frac{dN}{dt} = r_{\max} N, \text{ with no resource limitation.}$ $N_t = N_0 e^{\mu_{\max} t},$ $N_t = N_0 e^{r_{\max} t}.$ $\ln \left(\frac{N_t}{N_0} \right) = \mu_{\max} t.$ $\ln \left(\frac{N_t}{N_0} \right) = r_{\max} t.$ <p>EEOS630</p>	<p>Slide 39 The Malthusian parameter: r_{\max}</p> <p>NOTES:</p>

Specific growth rate, μ , and doublings per day (archaic)

in Units of inverse time

$$\ln \left(\frac{N_t}{N_0} \right) = \ln(2) = \mu t_d$$

$$t_d = \frac{\ln(2)}{\mu} \approx \frac{0.693}{\mu}$$

$$\text{Specific growth rate} \left[\frac{\text{doublings}}{\text{day}} \right] = \frac{1}{t_d}$$

$$= \frac{\mu}{\ln(2)}$$

$$\approx \frac{\mu}{0.693}$$

Slide 40 Specific growth rate, μ , and doublings per day (archaic)

NOTES:

Biomass-specific production, μ

Estimating biomass, in carbon, the key problem in estimating μ . Estimating photoautotrophic Carbon:Chl a ratio difficult

$$\mu = \frac{\text{specific production}}{\text{production}} = \frac{P}{B}$$

$$= \frac{\frac{dC}{dt}}{B}$$

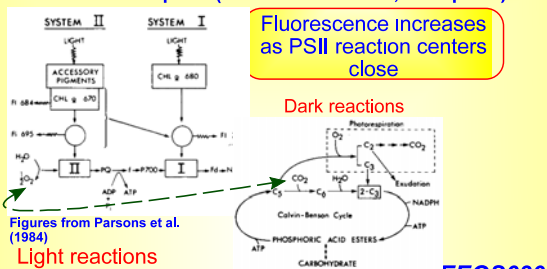
EEOS630

Slide 41 Biomass-specific production, μ

NOTES:

Gross primary productivity

Light-dependent rate of electron flow to terminal electron acceptors (Falkowski & Raven, 1997 p 264)



Slide 42 Gross primary productivity

NOTES:

Bell jars used to estimate O₂ flux

Uthicke & Klumpp (1998), MEPS

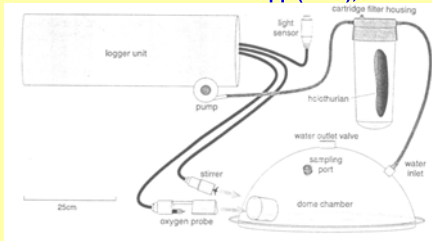


Fig. 1. Schematic diagram of the components of the respirometer with dome chambers as used in nutrient enhancement experiments. In routine respirometry measurements, the filter housing with holothurian was omitted. See Klumpp et al. (1987) for details on respirometer components

EEOS630

Slide 43 Bell jars used to estimate O₂ flux

NOTES:

O₂ flux used to measure Stellwagen Bank microphytobenthic production

Cahoon et al. 1993 Figure 1 & Conclusion

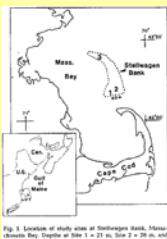


Fig. 1. Location of study area at Stellwagen Bank, Massachusetts Bay. Depth at site 1 = 25 m, site 2 = 30 m, and site 3 = 20 m.

The importance of benthic microalgal production at Stellwagen Bank derives from the apparent ability of the distinctly benthic microalgal assemblage there to sustain significant production at light levels consistently below 1% surface incident PPFD. If this ability is common, benthic microalgae may be widely distributed in continental shelf habitats. Benthic habitats underlying clearer, less productive water columns than at Stellwagen Bank may support relatively higher benthic microalgal production. Benthic microalgal production may therefore be a significant, if infrequently considered, fraction of total production in continental shelf ecosystems.

EEOS630

Slide 44 O₂ flux used to measure Stellwagen Bank microphytobenthic production

NOTES:

Redalje-Laws Chl *a* labelling

HPLC separation of Chl *a* to determine ¹⁴C activity
Gould & Gallagher (1990)

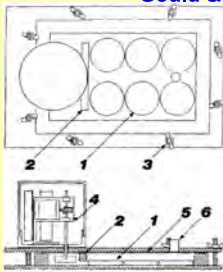


Table 1. Definitions and equations used in the ¹⁴C Chl *a*-labelling technique (adapted for sediments from Redalje and Laws 1981; Redalje 1983; Witschurkey and Lennarz 1984)

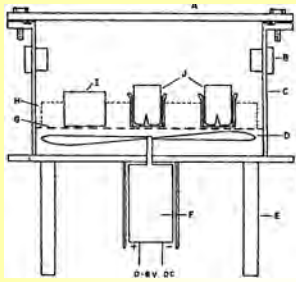
A^*	Activity of total particulate matter, dpm core ⁻¹
R^*	Specific activity of C in Chl <i>a</i> molecule, dpm μg ⁻¹ C
I^*	Specific activity of DIC, dpm μg ⁻¹ C
ΔC	C fixed during the incubation, μg C core ⁻¹ incubation ⁻¹ converted to μg C m ⁻² h ⁻¹
C_p	Microalgal C present at the end of the incubation, μg C core ⁻¹ converted to μg C cm ⁻²
μ	Specific growth rate per day assuming 12 h growth per day
1.05	Factor to account for isotope discrimination
t	Duration of incubation in hours
Equations:	
$\Delta C = 1.05 [A^* (I^*)^{-1} \times (1/t)]$	(1)
$C_p = A^* R^*$	(2)
$\mu = -\ln(1 - 1.05 R^* \times I^*) \times 12$	(3)

Slide 45 Redalje-Laws Chl *a* labelling

NOTES:

Sub-aerial production

Whitney & Darley's surveys of Georgia Salt marshes



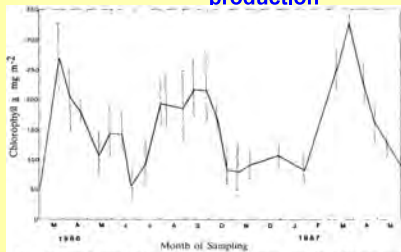
Georgia salt marshes
Highest benthic diatom production ever measured!
diffusive sublayer thickness < 10 μm

Slide 46 Sub-aerial production

NOTES:

Gould & Gallagher (1990)

Estimates of diatom standing stock, μ , and production



Slide 47 Gould & Gallagher (1990)

NOTES:

TABLE 4. RESULTS OF ^{14}C INCUBATIONS DONE IN SAVIN HILL COVE AND LABORATORY INCUBATION OF LUXURANT SEDIMENT. C: Chl ratio is based on Cp calculated via ^{14}C -Chl a labeling and on fluorometrically determined Chl a values. SD in parentheses. Spearman's rank correlation coefficients calculated for Savin Hill Cove data as follows: C: Chl ratio and μ , $r_s = -0.94$, $P < 0.01$; Cp and C: Chl, $r_s = 0.89$, $P < 0.05$; Cp and μ , $r_s = -0.78$, $P < 0.05$. Units given in Table 1. Temperature ($^{\circ}\text{C}$) in the incubation chamber at the end of the incubation—T; doubling time (d)—DT.

	T	μ	$P \times 10^3$	$P \times 10^3$	r_s	SD	$C_p \times 10^3$	μ	DT	C: Chl
Savin Hill Cove										
14 Aug 87										
Low tide	31	2.75	8.35(1.85)	8.56	489(31)	70(15)	3.23(0.98)	0.27(0.02)	2.6	21.3
30 Aug 87										
High tide	20	3.0	15.62(3.42)	7.60	346(11)	136(34)	8.51(2.21)	0.18(0.01)	3.9	32.5
11 Sep 87										
Low tide	28	3.0	3.76(0.41)	5.62	321(20)	44(3)	2.21(0.42)	0.24(0.02)	2.0	18.7
6 Mar 88										
Low-high	5	10.0	48.38(6.95)	8.59	593(66)	112(16)	15.40(3.36)	0.09(0.01)	7.7	54.4
19 Mar 88										
Low-high	7	11.0	28.49(5.43)	7.86	413(27)	65(13)	13.00(3.57)	0.06(0.01)	11.6	60.4
4 Jul 88										
Low tide	30	2.5	7.13(0.56)	5.75	192(08)	98(08)	6.19(0.89)	0.17(0.01)	3.9	42.5
4 Jul 88										
Low-high	20	10.5	18.55(0.20)	8.08	608(100)	69(04)	5.75(1.21)	0.15(0.03)	4.6	
Duxbury Beach										
7 Aug 88										
Lab	26	3.0	5.84(0.81)	7.14	95(09)	54(07)	11.60(3.00)	0.06(0.01)	11.6	55.4

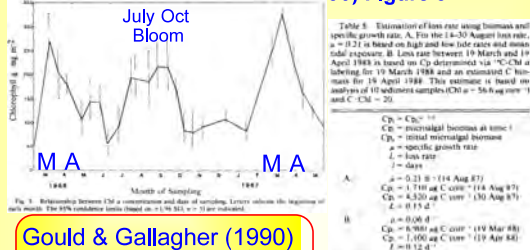
Doubling time = $\ln(2)/\mu \approx 0.69/\mu$

Slide 48

NOTES:

What causes the crash of the spring bloom?

Gould & Gallagher (1990) Figure 3



Gould & Gallagher (1990)
Grazing ($\approx 0.12 d^{-1}$)

Slide 49 What causes the crash of the spring bloom?

NOTES:

Serôdio & Catarino (2000)

O₂ microelectrodes & pulse amplitude modulated (PAM) fluorescence, dlver-PAM, <http://www.walz.com/>

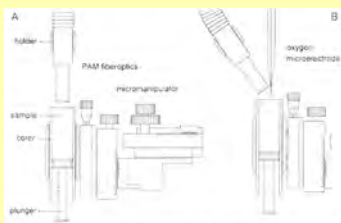


Fig. 1. The setup used for (A) measuring chl a fluorescence, using a PAM fluorometer, and for (B) measuring photosynthesis, using oxygen microelectrodes, on undisturbed microphytobenthic samples. When measuring photosynthetic rates, the PAM fiberoptic is used to illuminate the sample surface.

EEOS630

Slide 50 Serôdio & Catarino (2000)

NOTES:

Jørgensen & Revsbech (1985)

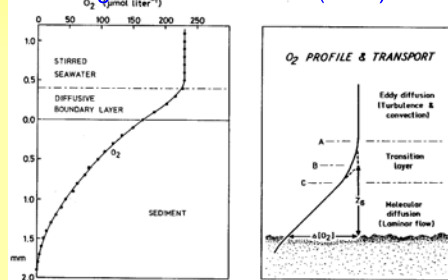


Fig. 1. Left. Oxygen microprofile in sediment collected from Aarhus Bay at 20-m water depth, July 1982. A transition (broken line) is seen above the sediment surface between the stirred seawater with homogeneous O₂ distribution and the diffusive boundary layer with a steep O₂ gradient. Right. The boundary layer at the sediment-water interface as determined by chemical transport processes and gradients. The oxygen microgradients are here used to define the outer limit (A) of the diffusive boundary layer as well as the true (C) and the effective (B) diffusive boundary layer.

Slide 51

NOTES:

Benthic boundaries

Ekman layer

Log layer

Viscous sublayer

Molecular diffusive sublayers

Ox c zone

Ox d zed zone

Sulfidogenic zone

Methanogenic zone

Slide 52

NOTES:

Thicknesses of benthic boundaries

Parameter	Deep-Sea	Shelf	Description
U (cm/s)	3	30	average water velocity
U_* (cm/s), boundary shear velocity	0.1	1	Boundary shear velocity (the square root of boundary shear stress/water density)
ν (cm ² /s)	2	200	characteristic eddy viscosity
z_i (cm)	500	5000	Ekman depth
z_l (cm)	100	1000	log layer thickness
z_v (cm)	2	0.2 to 1	viscous sublayer thickness
z_d (cm)	0.2	0.02-0.1	diffusive sublayer thickness $z_d = \sqrt{2D / (Sc^{1/2})}$, where Sc = Schmidt number $= \nu / \hat{D}$ 5-600 for O_2 or CO_2 \hat{D} = molecular diffusivity

Slide 53 Thicknesses of benthic boundaries

NOTES:

Revsbech & Jørgensen (1983)

O_2 microelectrode profiles of the best methods for estimating benthic primary production

Figure 3 shows four oxygen profiles (O₂ in μM) plotted against depth (cm) from 0 to 10. The profiles are labeled 'Light', 'Dark', 'Light', and 'Dark'. The 'Light' profiles show a sharp increase in O₂ concentration near the surface, while the 'Dark' profiles show a much lower, relatively constant O₂ concentration. The profiles are stacked vertically, with the 'Light' profile at the top and the 'Dark' profile at the bottom.

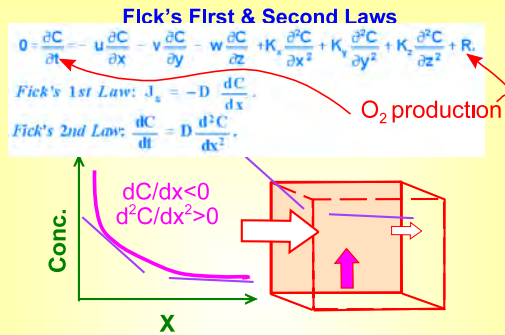
O_2 primary production obtained by subtracting the integrated light & dark profiles (after 1 min in dark)

EEOS630

Slide 54 Revsbech & Jørgensen (1983)

NOTES:

Advection-diffusion equation



Slide 55 Advection-diffusion equation

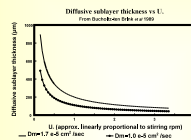
NOTES:

Stirring effects on diatom production

Stirred 0.23 d^{-1} (3-d doubling), Unstirred 0.11 d^{-1} (6 d)

Table 3. Results of stirred vs. unstirred incubation of mixed field populations collected 3 August 1987. SD in parentheses ($n = 3$). Units given in Table 1.

	μ^* ($\times 10^3$)	P^* ($\times 10^3$)	μ^*	P^*	C/D ($\times 10^3$)	μ
Stirred						
3.0	16.87(2.17)	1.41	764(43)	75(5)	4.16(0.82)	0.23(0.02)
Unstirred						
3.0	10.62(0.19)	1.34	356(32)	47(1)	5.62(0.67)	0.11(0.02)



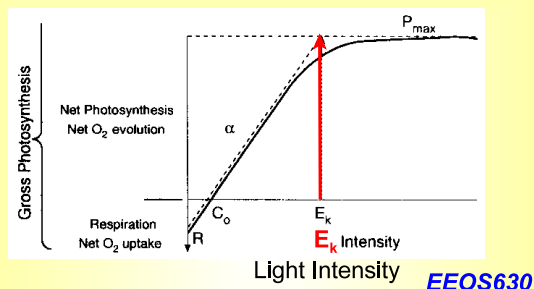
EEOS630

Slide 56 Stirring effects on diatom production

NOTES:

Falkowski & Raven P vs. E curves

Falkowski & Raven (1997, p. 196, Fig 7.2)



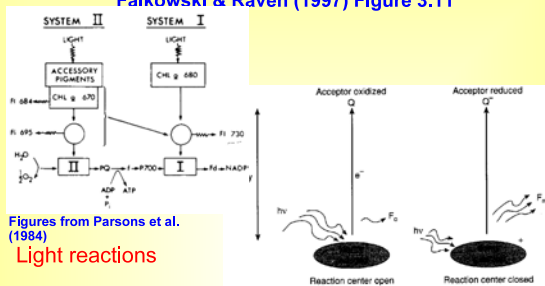
EEOS630

Slide 57 Falkowski & Raven P vs. E curves

NOTES:

Fluorescence yield and open & closed PSII reaction centers

Falkowski & Raven (1997) Figure 3.11

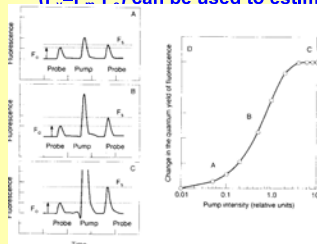


Slide 58 Fluorescence yield and open & closed PSII reaction centers

NOTES:

F_0 , minimal Chl a fluorescence (dark fluorescence)

Falkowski & Raven (1997): Pump intensities close PSII reaction centers. F_0 & differences in fluorescence ($F - F_0$) can be used to estimate production



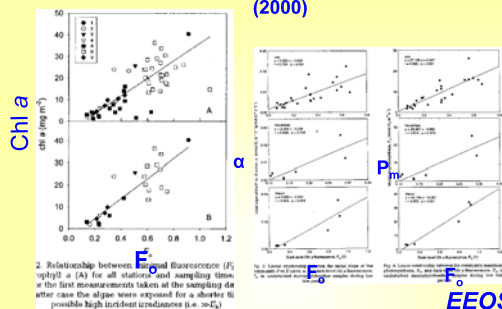
EEOS630

Slide 59 F_0 , minimal Chl a fluorescence (dark fluorescence)

NOTES:

F_0 linearly related to Chl a, α , & P_{max}

Barranquet & Kromkamp (2000), Serôdio & Catarino (2000)



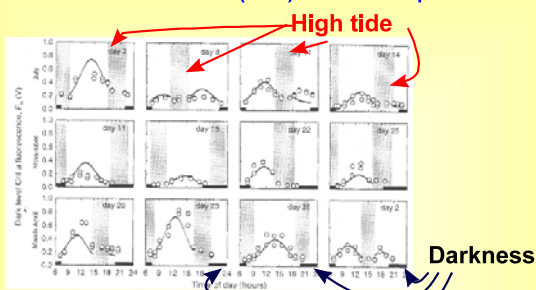
EEOS630

Slide 60 F_0 linearly related to Chl a, α , & P_{max}

NOTES:

Modeled effects of tide & light

Serôdio & Catarino (2000) Estimates of production

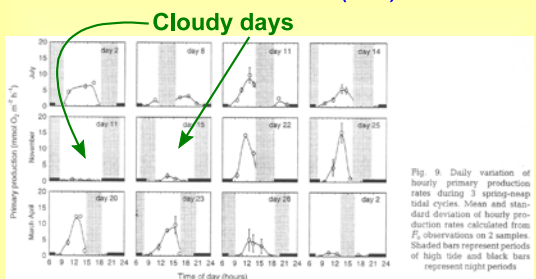


Slide 61 Modeled effects of tide & light

NOTES:

Modeled effects of tide & light

Serôdio & Catarino (2000)



EEOS630

Slide 62 Modeled effects of tide & light

NOTES:

Rates of diatom production

Epipelagic: about 100-200 gCm⁻²y⁻¹

Location/Source	Technique	g C/m ² /yr*	Author
<i>Benthic microalgae:</i>			
Georgia salt marsh	O ₂ , CO ₂	200	Pomeroy (1959)
Delaware salt marsh	O ₂	38-99	Gallagher and Daiber (1973)
California salt marsh	O ₂	215-400	Zedler (1980)
Massachusetts salt marsh	¹⁴ C (shaded)	106	Van Raaij et al. (1976)
<i>seagrass:</i>			
Intertidal sandflat	O ₂	143-225	Penneman (1968)
Intertidal sandflat	O ₂	6-325	Kirch and Phlips (1972)
Intertidal sandflat	¹⁴ C	4-9	Steele and Baird (1968)
Intertidal mudflat	¹⁴ C	31	Leach (1970)
Estuarine subtidal	¹⁴ C	116	Croome (1960)
	¹⁴ C	90	Marshall (1970)
	¹⁴ C	180	Joist (1978)
	¹⁴ C	58-177	Cadee (1980)
<i>Wadden Sea sand flat:</i>			
<i>Seagrass and mud flat:</i>			
Thalassia testudinum	O ₂	520-640	Westlake (1963)
Spartina (Georgia)	O ₂	257-897	Tied (1962)
(North Carolina to Nova Scotia)	cropping	130-256	Mann (1972b)
(Massachusetts)	cropping	1000-2300	Valiela et al. (1976)
<i>Mangrove swamps:</i>			
Florida (not prod.)	O ₂ (+ litter)	400	Mann (1972b)
<i>Epiphytes:</i>			
Laminaria (Nova Scotia)	cropping	1900	Westlake (1963)
(England)	cropping	1225	Bellamy et al. (1968)
(Nova Scotia)	blade renewal	1750	Mann (1972b)
Macrocystis	cropping	400-820	Cleland (1972)
<i>Littoral seaweeds:</i>			
Fucus	O ₂	<1000	Kaevliher (1966)

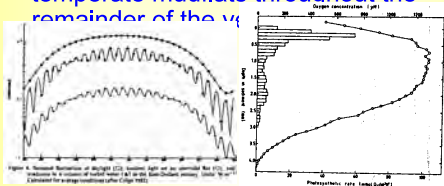
Slide 63 Rates of diatom production

NOTES:

What limits benthic production?

Light in winter, DIC in summer

- Production limited by light in winter
- Production may be limited by inorganic carbon in North temperate mudflats throughout the remainder of the year



Slide 64 What limits benthic production?

NOTES:

DIC limitation in diatoms mats

pH from Terry & Edyvean (1981)

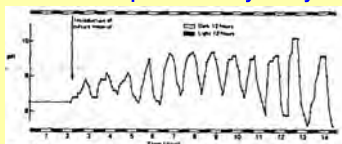
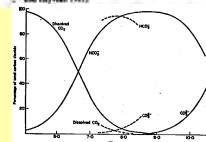


Figure 8. Time-course of pH change occurring under a mixed colonial diatom culture. (From Terry and Edyvean 1981)



Slide 65 DIC limitation in diatoms mats

NOTES:

pH & species composition

N. salinarum replaced by *N. pygmaea*

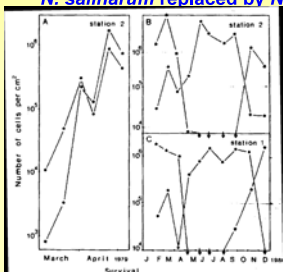


Fig. 3. Cell concentrations of *N. salinarum* (*) and *N. pygmaea* (●), calculated from total cell numbers and the relative species composition, during spring 1979 (A) and the year 1980 (B and C).

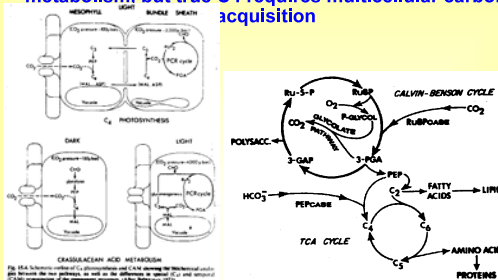
EEOS630

Slide 66 pH & species composition

NOTES:

Acclimation to low DIC

C3 and C4 photosynthesis; diatoms have a C4-like DIC metabolism, but true C4 requires multicellular carbon acquisition

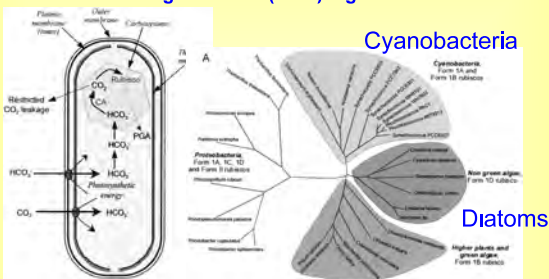


Slide 67 Acclimation to low DIC

NOTES:

Evolutionary History of DIC Concentrating mechanisms

Badger & Price (2003) Figs 1 & 2



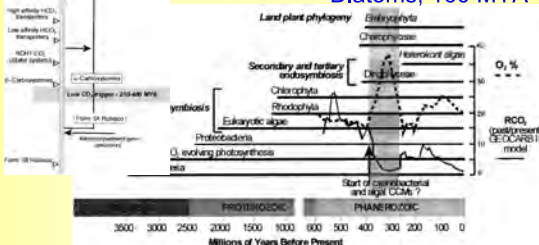
Slide 68 Evolutionary History of DIC Concentrating mechanisms

NOTES:

Cyanobacterial evolution & DIC concentrations

Badger & Price (2003) Figs. 7 & 8

Diatoms, 160 MYA

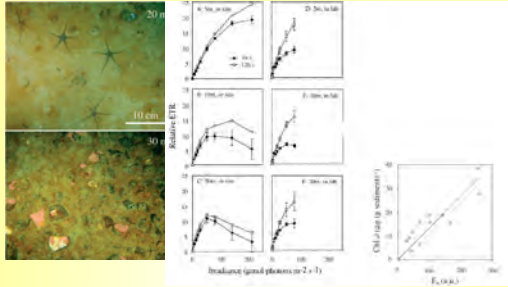


Slide 69 Cyanobacterial evolution & DIC concentrations

NOTES:

Measuring Production using fluorescence by SCUBA

Glud et al. 2002

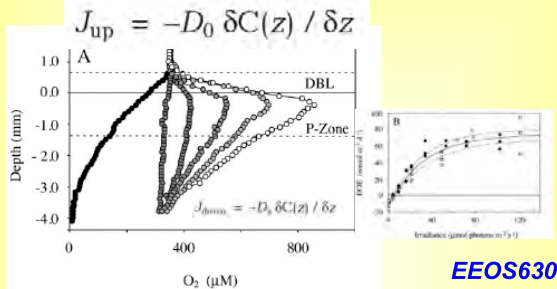


Slide 70 Measuring Production using fluorescence by SCUBA

NOTES:

Measuring production using fluorescence & O₂ flux by SCUBA

Glud et al. (2002) Figure 7

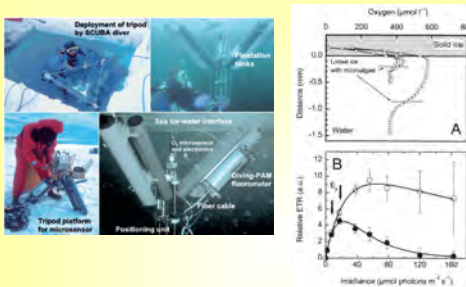


Slide 71 Measuring production using fluorescence & O₂ flux by SCUBA

NOTES:

PAM Fluorometer & O₂ microsensor

Kühl et al. 2002 MEPS 223: 1-14

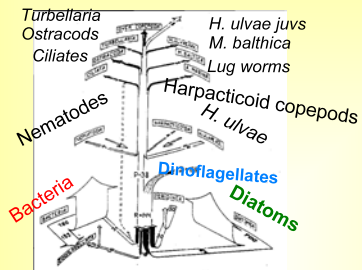


Slide 72 PAM Fluorometer & O₂ microsensor

NOTES:

Microphytobenthos: dominates benthic food supply

Slava Epstein's White Sea food web



EEOS630

Slide 73 Microphytobenthos: dominates benthic food supply

NOTES:

Herman et al. 2000

Linear relation between microphytobenthic production and infaunal biomass

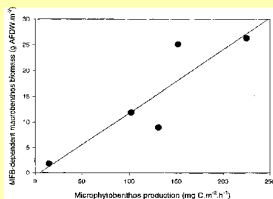


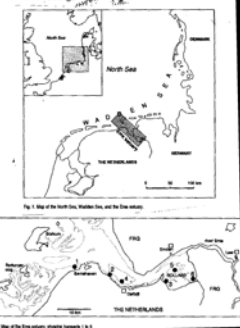
Fig. 8. Relation between microphytobenthic primary production (Hauke et al. 1998; C. Buitrago et al. 1999) and infaunal biomass that is calculated to be directly dependent on microphytobenthos (MPB) (see Table 2 for parameters and 'Discussion' for calculation). Linear regression coefficient is 0.54 (n = 5; p = 0.034). AFDW: ash-free dry wt.

EEOS630

Slide 74 Herman et al. 2000

NOTES:

Physical Processes and Dynamics of Microphytobenthos in the Ems Estuary (The Netherlands)



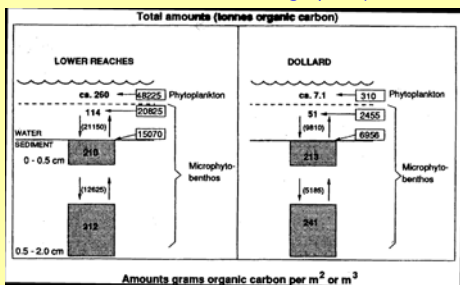
EEOS630

Slide 75

NOTES:

Photoautotrophic standing stock

From de Jonge (1994)



EEOS630

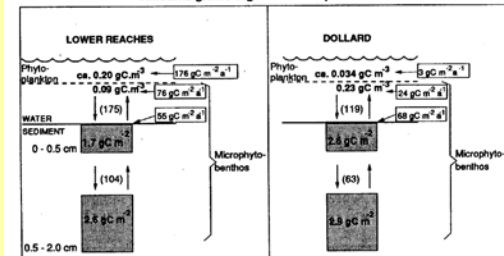
Slide 76 Photoautotrophic standing stock

NOTES:

Photoautotrophic production

From de Jonge

Amounts grams organic carbon per m² or m³



1977

10

Slide 77 Photoautotrophic production

NOTES:

Microphytobenthos & phytoplankton

- Ems Dollard
 - ▶ Microphytobenthic production 60-250 mgC m⁻² d⁻¹
 - ▶ 30% of phytoplankton are resuspended microphytobenthos
- Dollard (about 1 m deep)
 - ▶ 92% of Chl *a* from microphytobenthos
 - ▶ Production
 - 25% of total production from resuspended benthic diatoms
 - 53% from true phytoplankton
 - 22% from tidal flat production

EEOS630

Slide 78 Microphytobenthos & phytoplankton

NOTES:

Conclusions on microphytobenthos	Slide 79 Conclusions on microphytobenthos
<ul style="list-style-type: none"> • Microphytobenthic production is often a major source of labile organic matter in shallow benthic systems from the intertidal to approximately the 1% light depth (or slightly deeper) • Mucous production can have profound effects on sediment transport and organic geochemistry • Microphytobenthic production is intimately coupled to the physics of the benthic boundary layer • It can be measured using ^{14}C, O_2, or fluorescence • Benthic diatom specific growth is often very slow 	
	NOTES: